

## Effect of Ligand Deuteration on the Decay of $\text{Eu}^{3+}({}^5\text{D}_0)$ in Tris(2,2,6,6-tetramethyl-3,5-heptanedionato)europium(III)

Todd C. Schwendemann, Paul S. May, and Mary T. Berry\*

Department of Chemistry, University of South Dakota, Vermillion, South Dakota 57069-2390

Yuqing Hou and Cal Y. Meyers

Department of Chemistry and Biochemistry, Southern Illinois University, Carbondale, Illinois 62901-4409

Received: May 8, 1998; In Final Form: August 31, 1998

Contributions to the first-order rate constant for the decay of the  $\text{Eu}^{3+}({}^5\text{D}_0)$  state of tris(2,2,6,6-tetramethyl-3,5-heptanedionato)europium(III),  $\text{Eu}(\text{thd})_3$ , from radiative and multiphonon mechanisms are evaluated independently by measuring the luminescence decay rates in undeuterated  $\text{Eu}(\text{thd})_3$ , fully deuterated  $\text{Eu}(\text{thd}-d_{19})_3$ , and  $\alpha$ -deuterated  $\text{Eu}(\text{thd}-d_1)_3$ , which is also designated  $\text{Eu}(\alpha\text{-D,thd})_3$ . In the latter case, deuterium substitution is at the  $\alpha$ -carbon, between the carbonyl groups of the  $\beta$ -diketonate ligand. These measurements yield a multiphonon contribution of  $332\text{ s}^{-1}$ , of which  $157\text{ s}^{-1}$  is attributed to relaxation via the  $\text{C}_\alpha\text{-H}$  stretching vibration and  $175\text{ s}^{-1}$  to relaxation via the  $\text{C-H}$  stretching modes of the *tert*-butyl groups. By use of the measured total  $\text{Eu}^{3+}({}^5\text{D}_0)$  relaxation rate constant and the multiphonon rate constants given above, the  $\text{Eu}^{3+}({}^5\text{D}_0)$  radiative relaxation rate constant is inferred to be  $1930\text{ s}^{-1}$ . It is suggested that this unusually high radiative rate constant may be due to an increased allowedness in the  ${}^5\text{D}_0 \rightarrow {}^7\text{F}_j$  transitions due to contributions to the predominantly 4f crystal-field wave functions from a low-lying ligand-to-metal charge-transfer state.

### 1. Introduction

There is a considerable body of work assessing the importance of O–H oscillators in providing a nonradiative path for relaxation of the  ${}^5\text{D}_0$  state of  $\text{Eu}^{3+}$  ions in both solid state and in solution.<sup>1–3</sup> The high-energy O–H stretching mode provides an efficient path for electronic-to-vibrational energy transfer, an electronic-state relaxation mechanism generally referred to in solid-state materials as “multiphonon relaxation”. Much less work has been done to assess the importance of C–H groups on organic ligands to nonradiative relaxation. Notable exceptions include the work of Kropp and Windsor<sup>1</sup>, Dickens et al.,<sup>4</sup> and May et al.<sup>5,6</sup>

The C–H stretch is generally considered to be inefficient in relaxing the  $12\,000\text{ cm}^{-1}$   ${}^5\text{D}_0\text{--}{}^7\text{F}_6$  energy gap of  $\text{Eu}^{3+}$ , particularly when compared to the O–H stretch. This inefficiency is due largely to the lower energy of the vibration. Relaxation due to the C–D stretch ( $\bar{\nu} = 2100\text{ cm}^{-1}$ ) is expected to be negligible.<sup>7</sup> Dickens et al.<sup>4</sup> have assessed the contribution of ligand C–H oscillators to the decay of  $\text{Eu}^{3+}({}^5\text{D}_0)$  in two complexes with octadentate ligands based on 1,4,7,10-tetraazacyclododecane (see Figure 1a). For the first ligand, with the more closely associated methylene group, replacement of the methylene hydrogens with deuterium led to a decrease in the rate constant by  $26\text{ s}^{-1}$  per C–H oscillator. Replacing the more distant hydrogens at the benzylic position of the second ligand led to a decrease of only  $5\text{ s}^{-1}$  per C–H oscillator. Kropp and Windsor,<sup>1</sup> in an earlier work, found that, for 0.1 M aqueous ( $\text{D}_2\text{O}$ ) solutions of europium acetate, replacing acetate by perdeuterioacetate led to a decrease in the  ${}^5\text{D}_0$  decay constant from  $560$  to  $420\text{ s}^{-1}$ . Since the dominant solution species at that concentration should have been  $\text{Eu}(\text{OAc})_2^+$ , their results suggest a contribution of about  $23\text{ s}^{-1}$  per C–H group, which is quite consistent with the findings of Dickens et al.<sup>4</sup> May et al.,<sup>5,6</sup> using a measured decay constant of  $304\text{ s}^{-1}$  and a

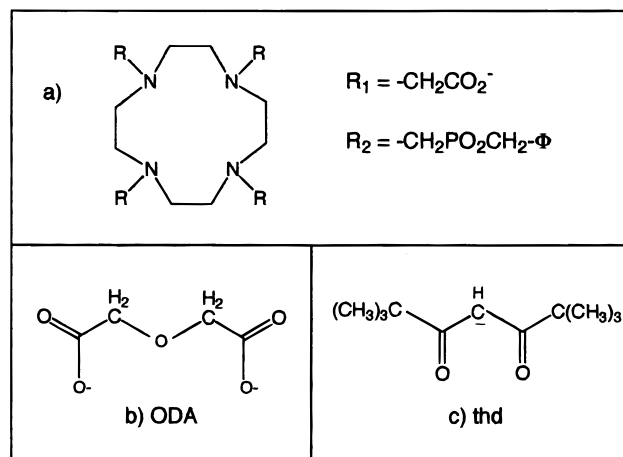


**Figure 1.** Structures for the (a) substituted 1,4,7,10-tetraazacyclododecane, (b) oxydiacetate, and (c) 2,2,6,6-tetramethyl-3,5-dionate ligands.

calculated radiative rate constant of  $94\text{ s}^{-1}$ , estimated that the ligand contribution to the decay rate of  $\text{Eu}^{3+}$  in  $\text{Eu}(\text{ODA})_3 \cdot 6\text{D}_2\text{O}$  was  $210\text{ s}^{-1}$ . If the ligand multiphonon decay can be attributed to the C–H stretch, which is the highest-energy vibration (see Figure 1b), an average contribution of  $18\text{ s}^{-1}$  from each of the 12 C–H oscillators is suggested, again consistent with the findings of Dickens et al.<sup>4</sup>

The  $\beta$ -diketonate complex, tris(2,2,6,6-tetramethyl-3,5-heptanedionato)europium(III) ( $\text{Eu}(\text{thd})_3$ ) is a particularly promising system in which to investigate the role of C–H oscillators in the nonradiative deactivation of  $\text{Eu}^{3+}({}^5\text{D}_0)$ . Although  $\text{Eu}(\text{thd})_3$  is hygroscopic and can form a monoquo adduct,  $\text{Eu}(\text{thd})_3 \cdot \text{H}_2\text{O}$ , the anhydrous form is used in this work, and therefore, no O–H oscillators are present in the crystal. The highest-energy vibration available is the C–H stretch at  $\sim 2900\text{ cm}^{-1}$ . There is one C–H

oscillator at the  $\alpha$  position and there are 18 on the *tert*-butyl groups of each of the ligands. Owing to their relative proximity, the  $\alpha$  oscillators might be expected to interact more effectively *per oscillator* with  $\text{Eu}^{3+}$  compared to the *tert*-butyl oscillators, but the large relative number of *tert*-butyl oscillators might result in their making a significant, collective contribution to non-radiative decay. In this work, the roles of the two different kinds of C–H oscillators in the deactivation of  $\text{Eu}^{3+}({}^5\text{D}_0)$  are assessed independently by selectively eliminating alternative paths of multiphonon relaxation by means of ligand deuteration. Total deuteration permits measurement of the radiative rate constant for decay of the  ${}^5\text{D}_0$  state.

In this work, we report the effect of deuteration of the thd ligand on the rate constant for  $\text{Eu}^{3+}({}^5\text{D}_0)$  relaxation in  $\text{Eu}(\text{thd})_3$ . The multiphonon contribution to the rate constant is  $332\text{ s}^{-1}$ , of which  $157\text{ s}^{-1}$  is attributed to relaxation via the  $\text{C}_\alpha\text{--H}$  stretching vibration and  $175\text{ s}^{-1}$  to relaxation via the C–H stretching modes of the *tert*-butyl groups. Using the measured total  $\text{Eu}^{3+}({}^5\text{D}_0)$  relaxation rate constant and the multiphonon rate constants given above, we have inferred that the  $\text{Eu}^{3+}({}^5\text{D}_0)$  radiative relaxation rate constant is  $1930\text{ s}^{-1}$ . That the residual rate constant is indeed radiative and not attributable to rapid energy migration to traps is confirmed by measurements in 0.5%  $\text{Eu}^{3+}$  doped into  $\text{Gd}(\text{thd})_3$ . This unusually high radiative rate constant may be associated with an increased allowedness in  ${}^5\text{D}_0 \rightarrow {}^7\text{F}_1$  transitions due to contributions to the predominantly 4f crystal-field wave functions from a low-lying ligand-to-metal charge-transfer state. The nature of this charge-transfer state in  $\text{Eu}(\text{thd})_3$  and its role in  ${}^5\text{D}_0$  relaxation at temperatures above 200 K have been discussed previously.<sup>8</sup>

## 2. Experimental Section

**2.1. Synthesis of 2,2,6,6-Tetramethyl-3,5-heptanedione- $d_{18}$  (thd- $d_{18}$ ).** The synthesis of thd- $d_{18}$  was accomplished as outlined in Figure 2. The preparations of pinacolone- $d_{12}$  and trimethyl- $d_9$ -acetic acid, starting from acetone- $d_6$ , were adapted from standard methods.<sup>9</sup> Following the general method for converting carboxylic acids into their chlorides,<sup>10</sup> trimethyl- $d_9$ -acetic acid was converted into pivaloyl chloride- $d_9$ , which was isolated and purified by fractional distillation; bp 104–105 °C [lit.<sup>11</sup> bp 105–106 °C for pivaloyl chloride]. To a solution of freshly distilled THF (50 mL) and LDA/THF–heptane solution (Acros Organics; 10.4 mL, 2 M, 20.8 mmol) maintained in an ice–water bath, pinacolone- $d_{12}$  (2.6 mL, 20.8 mmol) was added dropwise. After the mixture was stirred at 0 °C for 20 min, pivaloyl chloride- $d_9$  (1.3 mL, 10.4 mmol) was syringed in dropwise. The bath was removed, and the mixture was stirred at room temperature for 30 min and then transferred to a separatory funnel. The residue was washed with ether and the washings also transferred. The mixture in the funnel was washed with dilute HCl, and the organic layer was separated and dried over anhydrous  $\text{MgSO}_4$ . The mixture was filtered and the filtrate evaporated in vacuo, leaving a yellow oil (3.42 g). Column chromatography (silica gel, hexanes) provided thd- $d_{18}$ , 2.15 g, in about 75% yield ( ${}^2\text{H}$  NMR). A portion, 1.72 g, was dissolved in methanol and aqueous  $\text{CuSO}_4\text{--NaOAc}$  solution was added. The precipitated purple thd- $d_{18}$  Cu complex was extracted with hexanes, and the combined extracts were evaporated, leaving a purple solid, 1.63 g, which was recrystallized from 95% ethanol; 1.46 g, mp 192.5–193.5 °C [cor; lit.<sup>12</sup> 192–193 °C for thd–Cu complex]. This complex was dissolved in hexane (3 mL), 5 mL of 0.64 M  $\text{H}_2\text{SO}_4$  was added, and the mixture was stirred for 2 h. The aqueous layer was removed and extracted with hexane, and the extract was added to the organic layer. The latter was then

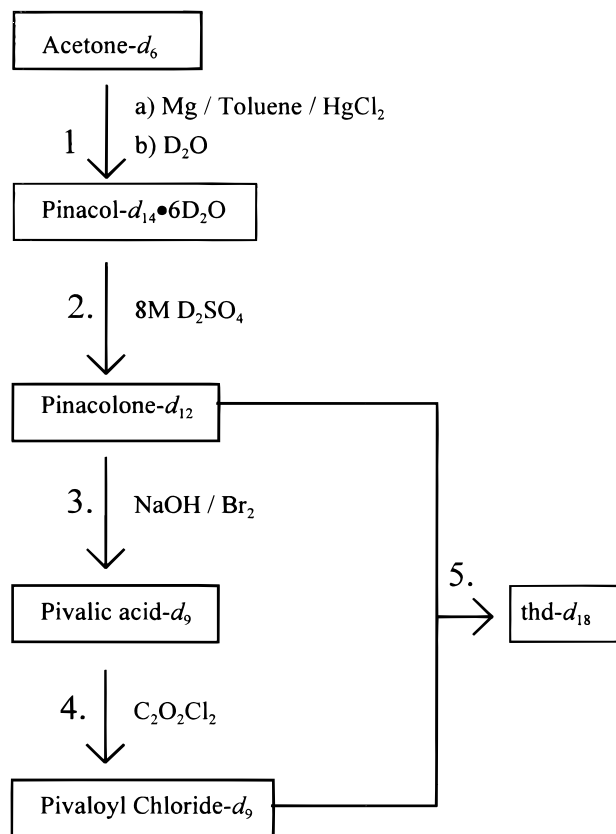


Figure 2. Synthetic route to thd- $d_{18}$ .

washed with 0.64 M  $\text{H}_2\text{SO}_4$ , and the hexane solution evaporated by passing dry  $\text{N}_2$  through it.

**2.2. Synthesis of the Europium Complex  $\text{Eu}(\text{thd-}d_{19})_3$ .** The synthesis of the complex was adapted from the method of Eisentraut and Sievers.<sup>13</sup> The ligand (6 mmol) was dissolved in 3 mL of EtOD. To this was added 0.245 g (6 mmol) of NaOD dissolved in 5 mL of 50/50 EtOD/ $\text{D}_2\text{O}$ . The solution was stirred at room temperature for 1 h. To this solution was added 0.733 g  $\text{EuCl}_3\cdot 6\text{H}_2\text{O}$  (2 mmol). A yellow precipitate formed immediately. To reduce the solubility of the complex in the EtOD/ $\text{D}_2\text{O}$  mixture, 10 mL of  $\text{D}_2\text{O}$  was added. The precipitate was filtered and dried at 50 °C under vacuum for 10 min, and the crude product was sublimed under vacuum at 125–175 °C for purification. The sublimed material showed a melting point at 187.5–188.0 °C (cor). The Aldrich Catalog lists 187–189 °C for  $\text{Eu}(\text{thd})_3$  (Resolve-A1).

**2.3. Synthesis of the Europium Complex  $\text{Eu}(\alpha\text{-D,thd})_3$ .** The complex with the ligand deuterated only at the methylene position was prepared as was the fully deuterated complex except that the ligand was the undeuterated form purchased from Aldrich. Efficient D/H exchange at the  $\alpha$ -position occurs in the NaOD/EtOD/ $\text{D}_2\text{O}$  solution prior to the addition of  $\text{EuCl}_3$ .

**2.4. FTIR Analysis of Materials.** FTIR spectra (Midac, M series) of undeuterated  $\text{Eu}(\text{thd})_3$  (Aldrich, Resolve-A1),  $\text{Eu}(\alpha\text{-D,thd})_3$ , and  $\text{Eu}(\text{thd-}d_{19})_3$  were measured in KBr (Aldrich, FTIR grade) pellets. These were used to confirm the level of deuteration in the complex.

**2.5. Luminescence Measurements.** The  ${}^5\text{D}_0 \leftarrow {}^7\text{F}_0$  laser excitation spectrum and the  ${}^5\text{D}_0 \rightarrow {}^7\text{F}_2$  emission spectrum were measured at room temperature and compared to previously measured spectra for undeuterated  $\text{Eu}(\text{thd})_3$ .<sup>8</sup> For both spectra, the excitation source was an  $\text{N}_2$ -laser/dye-laser combination (Laser Photonics UV-12/DL-14), using rhodamine 590 dye. Luminescence from the sample was collected using a single

*f*-matching lens focused at the entrance slit of a 0.46 m monochromator (Jobin Yvon HR460). Detection was achieved with a Hamamatsu R2949 photomultiplier connected to a Stanford Research Systems model SR430 multichannel scaler.

For the excitation spectrum, the monochromator was set for zeroth-order collection and the dye laser was scanned from 5750 to 5820 Å. Cutoff filters (610 and 590 nm) were used to eliminate laser scatter from the detection system. A 1.0 OD neutral density filter and narrow (2 Å) monochromator slits were used to reduce total signal. The laser was operated with the oscillator only (amplifier removed) for the same reason.

For the emission spectrum, excitation was fixed at 5787 Å, and the monochromator was scanned from 6050 to 6400 Å with 3 Å resolution. A 590 nm cutoff filter was used to eliminate laser scatter.

The experimental setup for measuring the  $^5D_0$  luminescence decay profiles and, hence, the  $^5D_0$  decay rates was similar to that used for measuring the excitation and emission spectra. The excitation was fixed on the  $^5D_0 \leftarrow ^7F_0$  transition (5787–5790 Å, shifting to longer wavelengths with lower temperatures), and emission was monitored on the  $^5D_0 \rightarrow ^7F_2$  transition at 6103 Å with 2 Å resolution. The time-resolved emission decay profiles were averaged over 1500 laser shots at the multichannel scaler and then downloaded to the controlling PC for analysis.

Temperature control (156–280 K) was achieved by mounting the sample on a heated copper rod in an optical Dewar, through which cooled N<sub>2</sub> gas was passed. The temperature was controlled by adjusting the N<sub>2</sub> flow rate and the voltage applied to the heater at the copper rod. Temperature was monitored using a chromel–alumel thermocouple.

Decay profiles were measured for Eu(thd-*d*<sub>19</sub>) between 156 and 271 K and for 0.5% Eu:Gd(thd)<sub>3</sub> at 208 K. Measurements for Aldrich Resolve-Al Eu(thd)<sub>3</sub>, which were reported in a previous work,<sup>8</sup> were repeated in the range 155–271 K. Decay profiles for Eu(α-D,thd)<sub>3</sub> were measured in the range 153–183 K.

### 3. Results and Discussion

**3.1. FTIR Analysis.** The FTIR spectrum of our synthesized Eu(thd-*d*<sub>19</sub>)<sub>3</sub> shows bands at 2211, 2124, 2074, and 2044 cm<sup>-1</sup> in the C–D stretching region. The region around 2900 cm<sup>-1</sup>, which is characteristic of the C–H stretch, shows no absorbance. The lack of absorbance in the 3500 cm<sup>-1</sup> region of the IR spectrum indicates that the sample is free of water.

The FTIR spectrum of our synthesized Eu(α-D,thd)<sub>3</sub> shows structure in the C–H stretch region identical to that of undeuterated Eu(thd)<sub>3</sub>. Furthermore, the spectrum is free of any features in the 2100 cm<sup>-1</sup> region that could be attributed to the C–D stretch. Two conclusions might be drawn from this information. First, there is the possibility that the α-position was not deuterated. However, if this were the case, there should also be no α-deuteration in our synthesized Eu(thd-*d*<sub>19</sub>)<sub>3</sub>, which would have resulted in a C–H stretch band near 2900 cm<sup>-1</sup> in the IR spectrum. A second possibility is that the C<sub>α</sub>–H/D stretch is not appearing in the expected region, or is simply too weak to be of use in assessing the degree of deuteration. Normal-mode analyses of the β-diketonate complexes Cu(acac)<sub>2</sub>, Pd(acac)<sub>2</sub>, and Fe(acac)<sub>3</sub> assign the C<sub>α</sub>–H stretch to the bands appearing at 3072, 3070, and 3062 cm<sup>-1</sup>, respectively,<sup>14</sup> but since the C<sub>α</sub>–H oscillator comprises only 1/19 or approximately 5% of the total C–H oscillators, the signal may be too weak to observe in our spectrum.

The 1500 cm<sup>-1</sup> region of the spectrum gives a more useful signature for α-deuteration. A closely spaced doublet, which

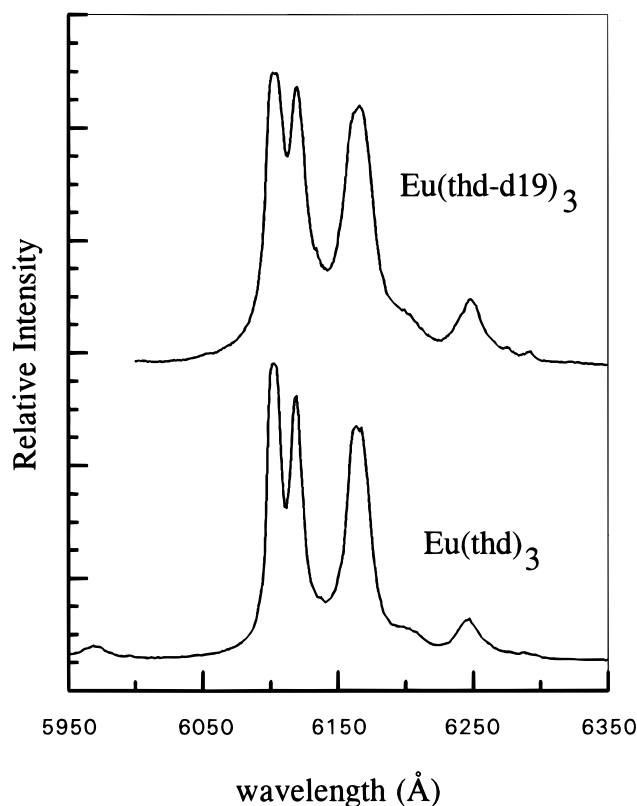


**Figure 3.** Comparison of the  $^5D_0 \rightarrow ^7F_2$  emission for fully deuterated and undeuterated Eu(thd)<sub>3</sub>. Excitation was set at 5787 Å on the  $^5D_0 \leftarrow ^7F_0$  transition. Emission resolution was 3 Å.

appears at 1540 cm<sup>-1</sup> in undeuterated Eu(thd)<sub>3</sub>, disappears in both Eu(α-thd)<sub>3</sub> and in Eu(thd-*d*<sub>19</sub>)<sub>3</sub>. A strong band, which appears at 1500 cm<sup>-1</sup> for the undeuterated material, is much reduced for the deuterated species, and a new peak appears at 1450 cm<sup>-1</sup>. By analogy to the acetylacetonate (acac) complexes, the 1540 cm<sup>-1</sup> band may be tentatively assigned to a C<sub>α</sub>–H out-of-plane bending combination and the 1500 cm<sup>-1</sup> band to a ring deformation mode involving principally C–C and C–O stretching. These coordinates are somewhat coupled to the C<sub>α</sub>–H in-plane bend in the acac complexes. A second indication is the in-plane C<sub>α</sub>–H bend, which is coupled to the C–CH<sub>3</sub> stretch and appears at 1189 cm<sup>-1</sup> in Cu(acac)<sub>2</sub>, at 1199 cm<sup>-1</sup> in Pd(acac)<sub>2</sub>, and at 1188 cm<sup>-1</sup> in Fe(acac)<sub>3</sub>. An analogous band appears at 1180 cm<sup>-1</sup> in Eu(thd)<sub>3</sub> but is much reduced in Eu(α-D,thd)<sub>3</sub> and Eu(thd-*d*<sub>19</sub>)<sub>3</sub>. Comparison of the relative intensity of this band in the deuterated and nondeuterated materials indicates 77% deuteration at the α-position for both Eu(α-D,thd)<sub>3</sub> and Eu(thd-*d*<sub>19</sub>)<sub>3</sub>. The hydrogens/deuteriums on the *tert*-butyl groups are not labile, and it is assumed that the degree of *tert*-butyl deuteration in Eu(thd-*d*<sub>19</sub>)<sub>3</sub> is the same as in the deuterated acetone (99.8% D) from which the ligand was synthesized.

**3.2. Emission and Excitation Spectra of Eu(thd-*d*<sub>19</sub>)<sub>3</sub>.** Both the  $^5D_0 \leftarrow ^7F_0$  excitation spectrum and the  $^5D_0 \rightarrow ^7F_2$  emission spectrum of Eu(thd-*d*<sub>19</sub>)<sub>3</sub> closely match the corresponding spectra reported previously for undeuterated Eu(thd)<sub>3</sub>.<sup>8</sup> The zeroth-order  $^5D_0 \leftarrow ^7F_0$  excitation spectrum shows a single peak at 5787 Å at room temperature. The  $^5D_0 \rightarrow ^7F_2$  emission spectra of the deuterated and undeuterated complex are shown for comparison in Figure 3. The spectral similarities, similar melting points, and similar sublimation characteristics strongly support the conclusion that our Eu(thd-*d*<sub>19</sub>)<sub>3</sub> is structurally similar to the undeuterated Eu(thd)<sub>3</sub>.

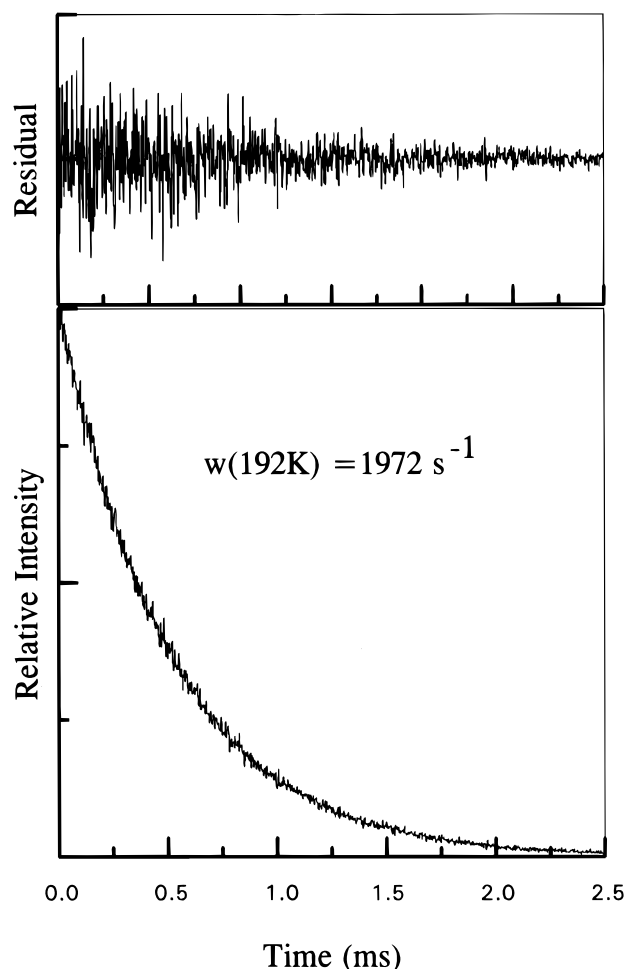


**Figure 4.** Luminescence decay profile for  $\text{Eu}(\text{thd-}d_{19})_3$  at 192 K. The residual shows the quality of fit to a single exponential of the form  $I_0 \exp(-1972 \times \text{time})$ .

**3.3.  $\text{Eu}^{3+}({}^5\text{D}_0)$  Relaxation Rates in  $\text{Eu}(\text{thd})_3$ ,  $\text{Eu}(\text{thd-}d_{19})_3$ ,  $\text{Eu}(\alpha\text{-D,thd})_3$ , and 0.5%  $\text{Eu}:\text{Gd}(\text{thd})_3$ .** All  ${}^5\text{D}_0$  luminescence decay curves measured in this study were found to be single-exponential. Figure 4 shows a decay profile for  $\text{Eu}(\text{thd-}d_{19})_3$  at 192 K with the residual of the fit to an exponential function.

The temperature dependence of the decay rate constants for  $\text{Eu}(\text{thd})_3$  and  $\text{Eu}(\text{thd-}d_{19})_3$  in the range 150–270 K is shown in Figure 5. Also included in Figure 5 is the rate constant measured for 0.5%  $\text{Eu}:\text{Gd}(\text{thd})_3$  at 208 K. As previously reported for undeuterated  $\text{Eu}(\text{thd})_3$ ,<sup>8</sup> the rate constants are relatively constant at temperatures up to 200 K, after which they begin to rise rapidly. The strong temperature dependence of the lifetime of the  ${}^5\text{D}_0$  state of  $\text{Eu}^{3+}$  in crystalline  $\text{Eu}(\text{thd})_3$  above 200 K has been attributed to relaxation through a low-lying ligand-to-metal charge-transfer state.<sup>8</sup> Owing to the significant thermal barrier to charge-transfer deactivation of  ${}^5\text{D}_0$  in  $\text{Eu}(\text{thd})_3$ , relaxation via this mechanism is ineffective below 200 K. Thus, at low temperatures, relaxation is due only to radiative and multiphonon processes.

Values for the low-temperature rate constants for  ${}^5\text{D}_0$  relaxation in  $\text{Eu}(\text{thd})_3$ ,  $\text{Eu}(\text{thd-}d_{19})_3$ ,  $\text{Eu}(\alpha\text{-D,thd})_3$ , and 0.5%  $\text{Eu}:\text{Gd}(\text{thd})_3$  are given in Table 1.

Multiphonon relaxation rates,  $w_{\text{mp}}$ , for lanthanides in a given host generally follow an exponential energy gap law,<sup>15–17</sup>

$$w_{\text{mp}} = \beta \exp(-\alpha(E - 2h\nu_{\text{max}}))$$

where  $E$  is the energy gap to be bridged,  $h\nu_{\text{max}}$  is the energy of

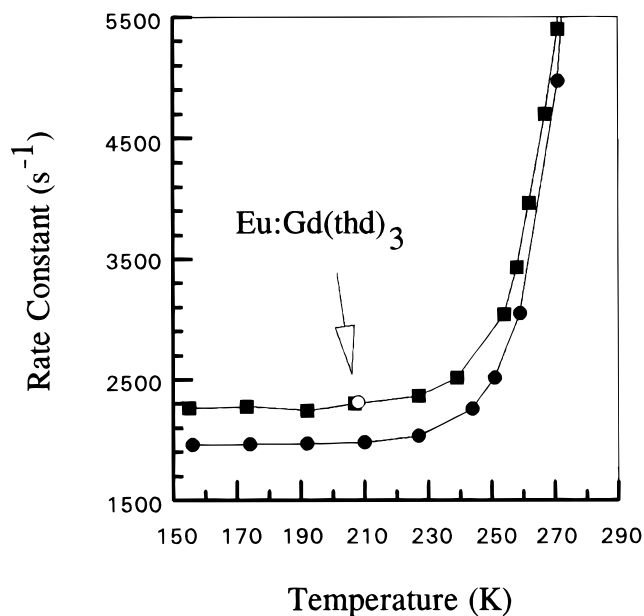


**Figure 5.**  $\text{Eu}^{3+}({}^5\text{D}_0)$  decay rate constants for undeuterated  $\text{Eu}(\text{thd})_3$  (square symbols),  $\text{Eu}(\text{thd-}d_{19})_3$  (closed circles), and 0.5%  $\text{Eu}:\text{Gd}(\text{thd})_3$  (open circle).

**TABLE 1: Low-temperature Rate Constants for  $\text{Eu}^{3+}({}^5\text{D}_0)$  Relaxation in  $\text{Eu}(\text{thd})_3$ ,  $\text{Eu}(\text{thd-}d_{19})_3$ ,  $\text{Eu}(\alpha\text{-D,thd})_3$ , and 0.5%  $\text{Eu}:\text{Gd}(\text{thd})_3$**

$\text{Eu}(\text{thd})_3^a$	$\text{Eu}(\text{thd-}d_{19})_3^a$	$\text{Eu}(\alpha\text{-D,thd})_3^a$	0.5% $\text{Eu}:\text{Gd}(\text{thd})_3^b$
$2262 \pm 9 \text{ s}^{-1}$	$1966 \pm 4 \text{ s}^{-1}$	$2141 \pm 6 \text{ s}^{-1}$	$2312 \text{ s}^{-1}$

<sup>a</sup> Mean values and standard deviations for the lowest-temperature measurements. <sup>b</sup> Value for measurement made at 208 K.

the highest-energy vibration available to the lanthanide, and  $\alpha$  and  $\beta$  are lattice-dependent parameters. Variation with host for  $\alpha$  and  $\beta$  is not large. Typical values for  $\alpha$  are on the order of  $10^{-2}$ – $10^{-3}$  cm. The parameter  $\beta$  is generally of the order  $10^7 \text{ s}^{-1}$ . Large energy gaps, like that between  $\text{Eu}^{3+}({}^5\text{D}_0)$  and the  ${}^7\text{F}_J$  manifolds, can be bridged efficiently only by high-energy vibrations. In  $\text{Eu}(\text{thd})_3$ , the highest-energy vibration is the C–H stretch of the thd ligand.

As mentioned previously, relaxation due to the C–D stretch is expected to be negligible. Therefore, the measured low-temperature rate constant in  $\text{Eu}(\text{thd-}d_{19})_3$  of  $1966 \pm 4 \text{ s}^{-1}$  is almost entirely radiative, except for a small nonradiative contribution due to incomplete deuteration at the  $\alpha$  position of the thd ligands. For  $\text{Eu}(\alpha\text{-D,thd})_3$ , the low-temperature rate constant is  $2141 \pm 6 \text{ s}^{-1}$ , which includes nonradiative contributions from the C–H oscillators of the *tert*-butyl groups. The low-temperature rate constant of  $2262 \pm 9 \text{ s}^{-1}$  measured in undeuterated  $\text{Eu}(\text{thd})_3$ <sup>18</sup> is due to radiative relaxation and nonradiative relaxation involving all the C–H oscillators of the thd ligand. The reported rate constants are averages of the three measured values for temperatures below 200 K. The errors represent the standard deviation of the mean.

The difference in the rate constants for  $\text{Eu}(\alpha\text{-D,thd})_3$  and  $\text{Eu}(\text{thd-}d_{19})_3$  gives the rate constant for the multiphonon path involving the C–H oscillators of the *tert*-butyl groups such that

$$w_{\text{mp}}(\text{tert-butyl C-H}) = 175 \pm 7 \text{ s}^{-1}$$

The difference between the rate constants for  $\text{Eu}(\alpha\text{-D,thd})_3$  and undeuterated  $\text{Eu}(\text{thd})_3$  gives the rate constant for the multiphonon path involving the  $\alpha$ -hydrogens (taking into

account that the  $\alpha$ -position is only 77% deuterated) such that

$$w_{\text{mp}}(\text{C}_{\alpha}\text{-H}) = 157 \pm 15 \text{ s}^{-1}$$

This gives a total multiphonon rate constant of  $332 \text{ s}^{-1}$  and an implied radiative rate constant of  $1930 \text{ s}^{-1}$ .

This radiative rate constant is unusually large for  $\text{Eu}^{3+}({}^5\text{D}_0)$ . The  ${}^5\text{D}_0$  radiative rate constants reported for other systems fall mainly in the range  $100\text{--}700 \text{ s}^{-1}$ . Such a large implied radiative rate constant might lead one to suspect that the residual rate constant is, in fact, not completely radiative and that some additional relaxation pathway has been overlooked. That there is no contribution to  ${}^5\text{D}_0$  relaxation due to rapid energy migration to (impurity) traps was established by measuring the rate constant in 0.5%  $\text{Eu}:\text{Gd}(\text{thd})_3$  at 208 K. This measurement gave  $w_{\text{total}} = 2312 \text{ s}^{-1}$  (see Figure 5), which is very similar to  $w_{\text{total}} = 2303 \text{ s}^{-1}$  measured for  $\text{Eu}(\text{thd})_3$  at 207 K.  $\text{Eu}^{3+}({}^5\text{D}_0) \rightarrow \text{Eu}^{3+}({}^5\text{D}_0)$  energy migration is extremely unlikely in the doped system, since the  $\text{Eu}^{3+}$  ions are, on average, too widely spaced. It is concluded, then, that the residual  $1930 \text{ s}^{-1}$  rate constant is indeed radiative.

A possible explanation for the unusually fast radiative rate may be related to the same phenomenon that causes very fast nonradiative decay at elevated temperatures.<sup>8</sup> If there is a low-lying ligand-to-metal-charge-transfer state, as postulated in ref 8, it is possible that the  ${}^5\text{D}_0$  state will have some small degree of charge-transfer character. A small contribution from the charge-transfer state to the predominantly 4f wave function of  ${}^5\text{D}_0$  could significantly enhance the allowedness of  ${}^5\text{D}_0 \rightarrow {}^7\text{F}_J$  transitions while having minimal effect on the position of the  ${}^5\text{D}_0$  energy level.<sup>19</sup> This explanation is also consistent with the unusually strong relative intensity of the  ${}^5\text{D}_0 \rightarrow {}^7\text{F}_0$  emission observed in  $\text{Eu}(\text{thd})_3$ .<sup>8</sup>

A summary of the contributions to the total rate constant for  ${}^5\text{D}_0$  relaxation in  $\text{Eu}(\text{thd})_3$  is given in Table 2. These values confirm the expectation that the efficiency of  $\text{Eu}^{3+}({}^5\text{D}_0)$  quenching by C–H vibrations is not as great as that by O–H vibrations but illustrate that, in instances where the C–H oscillators are closely associated, as in the  $\text{C}_{\alpha}\text{-H}$ , or numerous, as in the *tert*-butyl C–H, the effect can be significant.

#### 4. Conclusion

Relaxation of the  $\text{Eu}^{3+}({}^5\text{D}_0)$  state in  $\text{Eu}(\text{thd})_3$  at temperatures above 270 K is dominated by a temperature-dependent mechanism that has been attributed to deactivation through a ligand-to-metal charge-transfer state.<sup>8</sup> The dominant relaxation mechanism at low temperatures is radiative, but multiphonon relaxation via ligand C–H stretching vibrations is significant. The  $1930 \text{ s}^{-1}$  rate constant for radiative decay observed here is apparently the fastest reported for  $\text{Eu}^{3+}({}^5\text{D}_0)$ . It is speculated

**TABLE 2: Contributions to Total Rate Constant for  $\text{Eu}^{3+}({}^5\text{D}_0)$  Relaxation in  $\text{Eu}(\text{thd})_3$**

$w_r^a$	$w_{\text{mp}}(\text{C}_{\alpha}\text{-H})^b$	$w_{\text{mp}}(\textit{tert}\text{-butyl C-H})^c$	$w_{\text{CT}}^d$
$1930 \text{ s}^{-1} \pm 5$	$157 \text{ s}^{-1} \pm 15$	$175 \text{ s}^{-1} \pm 7$	$1.2 \times 10^{13} \text{ e}^{(-4100 \text{ cm}^{-1}/(RT))}$

<sup>a</sup> Radiative contribution to the rate constant. <sup>b</sup> Multiphonon contribution to the rate constant due to interaction with C–H oscillators at the  $\alpha$ -position of the thd ligand. <sup>c</sup> Multiphonon contribution to the rate constant due to interaction with C–H oscillators on the *tert*-butyl groups of the thd ligand. <sup>d</sup> Temperature-dependent contribution to the rate constant due to relaxation through a ligand-to-metal charge-transfer state. See ref 8.

that this large radiative rate is due to a small degree of charge-transfer character in the  ${}^5\text{D}_0$  state.

**Acknowledgment.** T.C.S. and M.T.B. thank Martin Hulse (Creighton University) and David Hawkinson (University of South Dakota) for suggesting a synthetic route to thd-*d*<sub>18</sub>. Acknowledgment is made to the donors of the Petroleum Research Fund, administered by the American Chemical Society for partial support of this project. Additional support was provided by the Research Corporation and the University of South Dakota.

#### References and Notes

- (1) Kropp, J. L.; Windsor, M. W. *J. Chem. Phys.* **1965**, *42*, 1599.
- (2) Lis, S.; Choppin, G. R. *Mater. Chem. Phys.* **1992**, *31*, 159.
- (3) Horrocks, W. DeW.; Sudnick, D. R. *J. Am. Chem. Soc.* **1979**, *101*, 334.
- (4) Dickins, R. S.; Parker, D.; de Souza, A. S.; Williams, J. A. G. *Chem. Commun.* **1996**, 697.
- (5) May, P. S.; Richardson, F. S. *Chem. Phys. Lett.* **1991**, *179*, 277.
- (6) May, P. S.; Metcalf, D. H.; Richardson, F. S.; Carter, P. C.; Miller, C. E. *J. Lumin.* **1992**, *51*, 249.
- (7) Haas, Y.; Stein, G. *J. Chem. Phys.* **1972**, *76*, 1093.
- (8) Berry, M. T.; May, P. S.; Xu, H. *J. Phys. Chem.* **1996**, *100*, 9216.
- (9) Furniss, B. S.; Hannaford, A. J.; Smith, P. W. G.; Tatchell, A. R. *Vogel's Textbook of Practical Organic Chemistry*, 5th ed.; Longman Scientific & Technical: New York, 1989; pp 527, 623, 669.
- (10) Fieser, L. F.; Fieser, M. *Reagents for Organic Synthesis*; Wiley & Sons: New York, 1967; Vol. 1, pp 767–769.
- (11) Rappoport, Z. *Handbook of Tables for Organic Compound Identification*, 3rd edition; CRC Press: Cleveland, OH, 1967; p 212.
- (12) Man, E. H.; Swamer, F. W.; Hauser, C. R. *J. Am. Chem. Soc.* **1951**, *73*, 901.
- (13) Eisentraut, K. J.; Sievers, R. E. *J. Am. Chem. Soc.* **1965**, *87*, 5254.
- (14) Mikami, M.; Nakagawa, I.; Shimanough, T. *Spectrochim. Acta, Part A* **1967**, *23*, 1037.
- (15) Engleman, R.; Jortner, *Mol. Phys.* **1970**, *18*, 145.
- (16) van Dijk, J. M. F.; Schuurmans, M. F. H. *J. Chem. Phys.* **1983**, *78*, 5317.
- (17) Schuurmans, M. F. H.; van Dijk, J. M. F. *Physica (Amsterdam)* **1984**, *12B*, 131.
- (18) Reference 8 reports  $w(T \leq 200\text{K}) = 2120 \pm 130 \text{ s}^{-1}$ , representing the 95% confidence limit. The large error bars were due to baseline anomalies in the digital oscilloscope used for that work.
- (19) Blasse, G. *Struct. Bonding* **1976**, *26*, 43.